

UPM 18030

Measurement of Heavy Oils Using Differential Pressure Meters

Craig Marshall, NEL

Abstract

Accurate flow measurement in heavy oils (below a Reynolds number of 2×10^4) is extremely difficult using traditional flow measurement technology. The fluids tend to be highly viscous (> 100 cSt), and cause an increase in frictional losses as Reynolds number decreases. The flow can also exhibit a variety of forms depending on the Reynolds number. For Reynolds numbers above 4×10^3 , the flow is generally considered turbulent; below 2×10^3 , the flow becomes laminar and in between these limits lies the transitional region characterised by dynamic and unpredictable mixtures of both laminar and turbulent flow.

Flow measurement of heavy oils using traditional differential pressure meters has been shown to have significant problems particularly in determining an accurate discharge coefficient and representative density to use in the calculation of mass flowrate. Due to the increase in frictional forces through the meter, typically caused by an increased fluid viscosity, the discharge coefficient is non-linear and reduces dramatically over a small Reynolds number region. Therefore, if the Reynolds number is not accurately known then potentially significant errors in flow measurement can be introduced (up to 40%).

A new method has been created based on differential pressure technology that can remove these errors by providing the Reynolds number in real-time and hence a corrected discharge coefficient. Furthermore, the inclusion of additional technology can also provide a calculation of the density and the viscosity of the fluid making it a 3-in-1 measurement solution. This is one of the first measurement techniques independent of operating Reynolds number making it ideal for heavy oil flow measurement.

Introduction

Heavy oils are characterised depending on their density rather than their viscosity [1]. Although there are various definitions for what constitutes heavy oil, it is commonly agreed that the majority contain impurities such as asphaltenes, waxes and carbon residue. The API gravity definition, a common definition used in the oil and gas industry worldwide, states that heavy oil has an upper limit

of 22°. Figure 1 shows the upper and lower limits of various categories of oil as stated in the API gravity definition.

Confirmed world oil reserves are split approximately into 70% high viscosity and 30% (low viscosity) conventional light oils. High viscosity oils are regarded as a vital energy resource for the foreseeable future, with significant yields forecast at 100 years or more.

A literature review conducted by NEL and Oxford University highlighted the issues facing application of conventional flow meters to high viscosity fluids [2]. Following on from the review, an initial experimental test programme [3] was instigated using a selection of conventional flow meters applied in viscous fluids. The overall conclusion from this work reinforced the notion that liquid flow meters cannot simply be relocated from low to high viscosity service without suitable characterisation or modification, nor can calibrations conducted in a low viscosity medium necessarily be applied to heavier crudes without appropriate compensation.

Differential pressure meters play a major role in conventional oil and gas production. However, it is widely known that they do not perform as well in high viscosity fluids owing to the increase in frictional forces within the meter [4-7]. This increase results in an increased sensitivity of the discharge coefficient to Reynolds number. Therefore, if the Reynolds number is not accurately known, then significant errors can be found in the overall flow measurement using the differential pressure flow meter. From ISO 5167-2 [8], a Reynolds number of 5,000 is the lowest applicable limit for a standard orifice plate.

There are some differential pressure meters that are used in low Reynolds numbers and are thought to be applicable through their linear discharge coefficient. These are quadrant edge orifice plates, conical entrance orifice plates and wedge meters. The use of quadrant edge and conical entrance orifice plates are detailed in ISO 15377:2007 [9]. However, there is a minimum Reynolds number even for these primary elements that limit their applicability and they will be shown to exhibit a non-linear discharge coefficient even within this range. Although thought to be very linear, wedge meter discharge

coefficient linearity at low Reynolds numbers has been found to be only partially true also [10].

In conventional oil and gas applications, the differential pressure meter is by far the most popular technology in terms of the number of units sold. There are a number of advantages that have facilitated this market share including cost, ease of use and calibration and maintenance requirements. In contrast, there is little evidence of a large commercial uptake of differential pressure meters for low Reynolds number applications [11]. This is primarily due to their poor performance caused by a non-linear discharge coefficient in low Reynolds numbers.

Owing to the many advantages of differential pressure meters, a solution to the non-linear discharge coefficient issue would result in substantially better measurement performance in lower Reynolds number applications in a cost-effective manner. A new method is presented here that can accomplish this task.

The new method will eliminate the Reynolds number effect within differential pressure meters (and other intrusive devices) allowing for an improved performance in low Reynolds number applications. In addition, there is potential to calculate the fluids physical properties in real-time through the addition of another measurement method. Case studies on Venturis and quadrant edge orifice plates will be shown.

Theory

Consider a typical discharge coefficient versus Reynolds number curve for a Venturi meter [4] as shown in Figure 2. Below a Reynolds number of 50,000, the discharge coefficient becomes increasingly non-linear with decreasing Reynolds number. Around the transition region, a hydraulic hump can be seen with an increase in discharge coefficient before it begins to fall off sharply again with decreasing Reynolds number into laminar flow.

This behaviour is typical in nearly all differential pressure meter types and can be seen in literature [4-7,10]. The shape is replicated in the very well used and well-known Moody plot which relates pipe friction factor to Reynolds number shown in Figure 3. Note the characteristic change in friction factor in turbulent to laminar flow in the critical zone highlighted in red.

The similarities suggest a link between friction factor and discharge coefficient which matches with theory as will be shown through equations 1 – 11.

Part 1: Real-time discharge coefficient trending

Consider equations 1 and 2, which show the Bernoulli equation and the differential pressure flow equations respectively. Bernoulli assumes inviscid flow i.e. a fluid with zero viscosity and links the dynamic, static and potential energies within the system. Equation 2 is derived from Bernoulli for an incompressible fluid and includes the discharge coefficient to account for differences from theory i.e. a real fluid with non-zero viscosity (amongst other differences).

$$\frac{p_1}{\rho g} + \frac{u_1^2}{2g} + z_1 = \frac{p_2}{\rho g} + \frac{u_2^2}{2g} + z_2 \quad (1)$$

$$Q_v = C_d \cdot \frac{\pi \cdot d^2}{4} \cdot \frac{1}{\sqrt{(1-\beta^4)}} \cdot \sqrt{\frac{2 \cdot (P_1 - P_2)}{\rho}} \quad (2)$$

Higher fluid viscosity increases the pressure drop through the meter and therefore increases the measured differential pressure. Or said another way, the higher the fluid viscosity, the less the measured pressure drop fully represents the change in static/dynamic energies through a restriction as predicted by Bernoulli.

It follows then, that as Reynolds number decreases (typically as viscosity increases) that the discharge coefficient should decrease to account for the added pressure drop caused by viscous friction. Friction factor plays an important role in this calculation and therefore it is clear that there is a relationship to discharge coefficient. Friction factor can be calculated through the Darcy-Weisbach equation, equation 3.

$$\lambda = \frac{2\Delta P_4 \cdot D}{\rho \cdot L \cdot u_D^2} \quad (3)$$

It is applicable across all Reynolds numbers and indications of friction factor values with respect to Reynolds number can be found in the Moody Plot (Figure 3). It's important to point out that in laminar flow the friction factor is independent of pipe roughness but this is not the case in turbulent flow.

Friction factor is dependent on system geometry, the fluid velocity and fluid density with the primary measurement being the pressure drop along a straight length of pipe. The calculation of flow rate through a restriction and friction factor both require a measurement of differential pressure as the primary measurement point. Consider the following meter set up as shown in Figure 4.

From (3), friction factor is dependent on pipe velocity squared. Rearrange (2) in terms of pipe velocity gives (4) and squaring (4) results in (5).

$$u_D = C_d \cdot \beta^2 \cdot \frac{1}{\sqrt{(1-\beta^4)}} \cdot \sqrt{\frac{2 \cdot (\Delta P_1)}{\rho}} \quad (4)$$

$$u_D^2 = \frac{2 \cdot C_d^2 \cdot \beta^4 \cdot \Delta P_1}{\rho(1-\beta^4)} \quad (5)$$

Inserting (5) into (3) and rearranging yields a new equation for friction factor that is independent of physical properties (6).

$$\lambda = \frac{\Delta P_4}{\Delta P_1} \cdot \frac{C_g}{C_d^2} \quad (6)$$

Where,

$$C_g = \frac{D(1-\beta^4)}{L \cdot \beta^4} \quad (7)$$

The relationship between friction factor and Reynolds number is well known for both laminar (8) and turbulent flows (9 – Colebrook-White). Once friction factor is calculated so too can Reynolds number be obtained.

$$\text{Re} = \frac{64}{\lambda} \quad (8)$$

$$\frac{1}{\sqrt{\lambda}} = -2 \log \left(\frac{\varepsilon}{3.7D} + \frac{2.51}{\text{Re} \sqrt{\lambda}} \right) \quad (9)$$

From calibration, standard equations or other, the relationship between discharge coefficient and pipe Reynolds number can be obtained and the appropriate discharge coefficient can then be calculated.

Knowing the relationships between the parameters, each measurement can calculate the corrected discharge coefficient and Reynolds number of the flow instantaneously. This allows for the effect of Reynolds number to be eliminated using two differential pressure measurements alone.

The Reynolds correction method will work for all intrusive type flowmeters that cause a repeatable,

reproducible and measurable pressure drop. Differential pressure meters have been focused on in this paper due to their lower cost, however, future work will show the method with other intrusive style meter e.g. turbines, Coriolis etc.

Part 2: Real-time physical property calculations

The new method can be taken further still by including another measurement technique alongside the differential pressure measurement system. Figure 5 provides the example of the set up using a clamp-on ultrasonic meter in the straight length of pipe upstream of the meter. Other technologies can be used in a similar method.

Rearranging (3) in terms of density provides (10). The velocity input in (10) is provided by the clamp-on ultrasonic measurement.

$$\rho = \frac{2\Delta P_4 \cdot D}{\lambda \cdot L \cdot u_D^2} \quad (10)$$

The calculated density from (10) can then be used in (2) for calculation of volume flow rate (or alternatively rearranged for mass flow rate or velocity) with previous calculation of the correct discharge coefficient.

In addition, with knowledge of density, velocity and Reynolds number it is possible to calculate viscosity of the fluid through (11).

$$\mu = \frac{\rho \cdot u_D \cdot D}{\text{Re}} \quad (11)$$

During calibration, correction factors can be obtained and then applied in operation as per standard practice for any stage in the calculation process. For differential pressure meters, the above theory (Parts 1 and 2) will provide a Reynolds number corrected flow measurement with physical properties estimates in real-time. However, for physical properties estimations it does require an additional measurement method i.e. clamp-on ultrasonic meter. Alternatively, a densitometer itself could be used in the system instead of velocity device. This will provide a lower uncertainty solution for flow, density and viscosity.

Using the method with another intrusive style flow measurement device e.g. turbine, positive displacement or Coriolis, will result in the same output without the requirement for a secondary technology. An intrusive meter plus the two differential pressure measurements will deliver flow, density and viscosity in real-time – a major

advantage in heavy oil applications and for a lower cost than having 3 separate instruments.

Testing

Figure 6 provides a schematic diagram of the heavy oil flow test facility at NEL in the UK which is accredited by United Kingdom Accreditation Service (UKAS). The heavy oil facility is a nominal 8 inch diameter test section capable of providing flowrates of up to 540 m³/hr of viscous fluids up to 1500 cSt. The facility can be modified to suite any meter size.

For 'primary' calibrations, a gravimetric 'standing-start-and-finish' method is used to determine the quantity of fluid (volume or mass) that has passed through the flow meter under test and into the selected weight tank.

The gravimetric weight tanks constitute the primary reference standard of the NEL oil flow facility. Using the above technique, the overall uncertainty in the reference flow rate, expressed at the 95% confidence level is 0.03 % ($k = 2$).

For a 'secondary' calibration, the quantity of oil passing through the test meter is measured using a pre-calibrated positive displacement reference meter, installed in series with the device under test. The reference meters used at NEL have a history of previous calibrations and uncertainties of the order of 0.25 % ($k = 2$) in fluids above 50 cSt.

Other reference quantities such as density and viscosity are taken using offline laboratory correlations against temperature and measuring the temperature during test points. The uncertainty in density and viscosity is estimated to be 0.02% and 2% ($k=2$) respectively.

Several differential pressure meters were tested with the new method with successful results. Six Venturis of nominal diameter between 4 and 8 inch and betas of 0.4, 0.6 and 0.75 were used as well as two 8 inch quadrant edge orifice plates of beta 0.45 and 0.6. For all testing, the Reynolds number range was roughly 100-15,000 and was achieved through testing at three temperatures spanning the range of 12 °C up to 40 °C which resulted in a range of viscosities. The test fluid was Aztec. The straight length of pipe used was roughly 10 D in each case.

Figures 7-11 show the discharge coefficient versus Reynolds number curves for the meters. Owing to the shape of the curves generated, there is no single curve that sufficiently represents each meter (except $\beta=0.4$ Venturis). For each meter, a curve was fitted to each flow regime i.e. one for laminar and one for turbulent. During transition, a simple assumption that the discharge coefficient would be an average of the two curves was used. More complex

algorithms can be applied. It is important to note that the point of transition from either laminar to turbulent or vice versa is not constant for a particular meter but is dependent on the current operating conditions i.e. the transition point will change from laboratory to the field.

For the Venturi meters there is a clear trend in results that all meter geometries follow. Reducing Reynolds number from 10,000 shows a gradually decreasing discharge coefficient until the fluid reaches the transition point. In the majority of the cases shown this is around a Reynolds number of 3,000 – 4,000. At this point, there is a sharp increase in discharge coefficient (hydraulic hump); the magnitude of this increase is proportional to beta where a larger beta results in a larger increase. Once the discharge coefficient reaches a maximum ~2,000 Reynolds number it begins to decrease again in a steeper manner.

Noticeable differences from the above generic description is shown in Figure 8 for the 6 inch $\beta=0.75$ Venturi where the start of transition appears at a larger Reynolds number. The increase in discharge coefficient is no longer sharp and is indicative of a larger transition region than seen in the 8 or 4 inch tests.

In addition, the results of the $\beta=0.4$ Venturis show a removal of the increase in discharge coefficient completely. This suggests that smaller betas help smooth out the change between different flow regimes. Considering the comparison of pipe to throat Reynolds numbers around the transition point suggests that lower betas will reduce the effect of changing flow regimes i.e. there is a larger Reynolds range where the pipe will be laminar and the throat will be turbulent.

For the orifice plates shown, both show similar trends in results that mimic the Venturi data only at different magnitudes. Both plates have a linear discharge coefficient in turbulent flow giving credence to the claimed performance in low Reynolds numbers. At some critical Reynolds number, there is an increase in discharge coefficient that reaches a maximum and then reduces with further reducing Reynolds number.

The vertical dotted line (blue) in Figures 10 and 11 indicates the minimum Reynolds number the discharge coefficient equation found in [9] can be applied for that meter geometry. The horizontal dashed line (red) is the value expected from [9] for discharge coefficient and the horizontal dotted lines (black) are the 2% uncertainty in the discharge coefficient calculation.

Again, the larger beta provides a larger increase in discharge coefficient at transition, similar to the Venturis. For

the $\beta=0.6$, the increase occurs below the minimum Reynolds number and the meter performs as expected from the specification in [9]. For the $\beta=0.45$, the increase in discharge coefficient occurs above the minimum Reynolds number and some discharge coefficient values fall outside the 2% uncertainty bands. This indicates that the equations found in [9] may not meet the stated performance levels and should be reviewed. It is thought the equations were derived from data acquired in the 1940's which have subsequently been lost.

Concentrating on the 8 inch $\beta=0.6$ quadrant edge orifice plate, and applying the new method shows some interesting results. For laminar flow, the discharge coefficient was fitted to an exponential function of Reynolds number and turbulent flow utilised the equation in [9] with an offset applied. The Reynolds number itself was calculated from equation 8 for laminar flow and the Colebrook-White equation (equation 9) for turbulent flow. A relative surface roughness of 0.05 mm was assumed.

Figure 12 shows the friction factor versus Reynolds number for a variety of calculation methods. From the reference data recorded, the new calculation method (equation 6) provides the same numerical answer as using the Darcy-Weisbach equation (equation 3). However, in comparison to theory i.e. equations 8 and 9, there are errors.

The error in the calculated friction factor is repeatable in both laminar and turbulent flow and can be corrected to remove the bias. It is important to note the new method under predicts in both laminar and turbulent flows with turbulent flow being significantly larger.

Having the ability to calculate friction factor and therefore Reynolds number, and knowledge of the correlation between discharge coefficient and Reynolds number it is possible to iterate the three to satisfactory solutions.

Figures 13, 14 and 15 show the errors in the results for discharge coefficient, Reynolds number and volume flow rate versus Reynolds number using the new method. Knowledge of the fluid density is required for the flow rate calculation.

The error in predicted discharge coefficient is reasonably good across most Reynolds numbers with the majority of points within 0.2% error. However, below 3,250 Reynolds number there is a noticeable increase in error. Remember the minimum Reynolds number this orifice geometry is said to operate to is 3,250 so this error is justified. The reason for the increase in error is due to the hydraulic hump that causes an increase in discharge coefficient which is not captured in the ISO equation.

This emphasises the importance of operating meters within their stated ranges. In a typical field application, this plate could have been used outside its specified range very slightly which would introduce an almost 1% under-reading error in flow rate.

The error in calculated Reynolds number is within 5% for all but 3 points. The error in laminar flow is better than turbulent flow with a much lower spread in results. In turbulent flow, the Reynolds number is derived using the Colebrook-White equation (applicable at $Re > 4,000$) which has an uncertainty of 10%. Other simpler or more complex correlations are available but have not been applied to this data.

The error in volume flow rate is essentially similar to the error in discharge coefficient as the reference density was used in its calculation. Other parameters are essentially constants in the equations.

Taking the results further with the inclusion of a liquid clamp-on ultrasonic meter, it is also possible to calculate the physical properties in real-time, creating a 3-in-1 meter. Calibrating the clamp-on ultrasonic meter against Reynolds number allowed for the uncertainty in velocity measurement to be reduced

The velocity measurement was used to calculate the density of the fluid from equation 10, which was then used in another calculation of volume flow rate. Figures 16, 17 and 19 show the errors in calculated density, volume flow rate using the calculated density, and the fluid viscosity versus Reynolds number respectively.

The error in density is within 2%, with the major contribution to this error being the clamp-on ultrasonic meter. Using a more accurate device will result in a reduced error.

The error in volume flow rate using the calculated density is within 1%, with most points within 0.5%. The larger errors associated with the discharge coefficient are not as noticeable in this example as the error in density has worked to counteract its effect.

Lastly, the errors found in the calculation of dynamic viscosity are essentially mirror images of the error in calculated Reynolds number, with that being the major component in its calculation. Again, the majority of calculated viscosity errors are within 5% of the reference value.

Discussion

One of the primary measurement issues in low Reynolds number applications is the dependence of the performance

index (e.g. discharge coefficient, K Factor, Meter Factor etc) on the Reynolds number itself. With a non-linear performance index any errors in the assumed Reynolds number can result in large errors in flow rate. This is true for the majority of flow measurement devices including differential pressure, turbines, Coriolis and ultrasonic meters. The difficulty comes through a requirement to know Reynolds number in order to apply the appropriate correction. However, if Reynolds number is known, then the user will probably have knowledge of flow rate already and therefore may not require the flow meter in the first place.

This new measurement method alleviates this problem by offering real-time knowledge of Reynolds number resulting in a more accurate performance index e.g. discharge coefficient for differential pressure meters, that can be applied to correct the flow rate. This paper has focussed on differential pressure flow meters but the theory can be applied to any technology that causes a repeatable, reproducible and measureable pressure drop caused by a restriction in the flow to offer a Reynolds number correction.

The method is based on a pressure loss over a straight length of pipe. To achieve a measurement with low uncertainty, it is advantageous for the pipe pressure loss to be as high as possible to increase resolution and reduce the turndown effect (zero errors). From equation 3, the only parameter that is variable for each installation is the length of pipe, L . A larger L results in a larger pressure drop and therefore L must be sized to ensure a measurable pressure drop is achieved with low uncertainty. Fortunately, in highly viscous fluids, the pipe pressure drop is larger than in less viscous fluids which can reduce the pipe length required.

In these tests, a pipe length of at least $10 D$ was included with reasonable results. Considering standard installation recommendations for upstream straight lengths of pipe of differential pressure meters, this value is certainly not excessive.

Another factor for discussion is on the critical Reynolds numbers for transition from laminar upwards and turbulent downwards. As discussed, this is not a fixed number and will vary from fluid to fluid, temperature to temperature and installation to installation. A full understanding of this phenomena is not yet available. The fact that this point is not static though puts in to question current calibration methods.

The current practice is to calibrate a meter over a specified range to determine its performance. The assumption is then that the meter will operate the same way in operation. One method of removing the effects of different fluids, physical properties, temperatures etc is to calibrate against Reynolds number. From empirical data and theory, matching

Reynolds number is a valid method and results with low uncertainty can be obtained. This works in higher Reynolds numbers as the characteristic performance of the meter does not change at the same Reynolds numbers created from different conditions i.e. the relationship is fixed.

In lower Reynolds number, and specifically in the transition region, the relationship is not fixed and can change depending on the critical Reynolds number when entering transitional flow. For differential pressure meters, this means that performing a calibration in one fluid and deriving the discharge coefficient relationship with Reynolds number may not be valid over a small range. For instance, if during the calibration the transition region was found to be 2,100-3,000, and in operation it was found to be 2,500 – 4,500, then there would be a mis-match to some degree of calibrated discharge coefficient to the actual discharge coefficient. Fortunately, this would only be a small range and any error would be proportional to the differences between laminar and turbulent flow performance and hence a function of beta.

Operation of this new method in higher Reynolds numbers (without the additional technology) becomes less practical as friction factor approaches the fully turbulent line of the Moody plot (Figure 3). The sensitivity of determining Reynolds number from friction factor becomes lower until Reynolds number is entirely independent of friction factor. However, when this occurs, the Reynolds number is sufficiently high that the discharge coefficient tends to attain linearity again and Reynolds effects become negligible (compared with low Reynolds number applications) i.e. there is no significant need for knowledge of Reynolds number to counter Reynolds effects.

The inclusion of another measurement technique into the system offers additional advantages across a wide range of Reynolds numbers. In this paper, a clamp-on ultrasonic meter was used but any other velocity or density measurement device could be substituted with similar results. In low Reynolds number applications, this will provide both density and viscosity of the flowing fluid in real-time which offers substantial benefits to end-users.

Lastly, there are still areas of research to explore for this new method which will be conducted in the near-future. Specifically, more focus will be placed on:

- Critical Reynolds number effects e.g. changing fluids
- Developments in higher Reynolds numbers
- Combining the method with other technologies
- Developments in two and three phase flows
- Development of standard equations in laminar flow
- Investigating equations in ISO 15377:2007

- Calculation of uncertainty

Conclusions

This paper has presented a new method, based on differential pressure measurements, to provide a Reynolds number correction for intrusive type flow meters. The focus has been on differential pressure flow meters due to the many advantages they offer, which have led to a large market share in conventional applications. However, any intrusive flow meter offering a repeatable, reproducible and measureable pressure drop can use the method.

Heavy oil production is an important application for future energy needs with a lot of associated measurement challenges. In heavy oil production, there are numerous measurement requirements from general process measurement through to fiscal level accuracy. Specifically, there is a need for a cost effective general process measurement device with uncertainty in the region of 2% and this new method can offer a solution to fill this gap.

For the meter presented, the error in Reynolds number was within 5%, the error in discharge coefficient was within 0.2% and the error in volume flow rate was within 0.2% (using a known density).

Utilising an additional measurement technique in combination with the new method provides calculation of fluid density to within 2%, fluid viscosity to within 5% and volumetric flow rate to within 1% (using the calculated density).

There are areas of development to deliver a complete solution in low Reynolds numbers using this method but the work presented highlights its current capabilities.

Acknowledgements

The author wishes to thank NEL for the opportunity to complete this doctorate research, NEL staff for their help and guidance and Coventry University for their input and supervision through the doctorate programme.

Nomenclature

P	=	Static Pressure
ρ	=	density
g	=	Gravitational constant
u	=	Velocity
d	=	Throat diameter
D	=	Pipe diameter
β	=	Ratio of throat to pipe diameter
λ	=	Darcy-Weisbach friction factor
ΔP_1	=	Pressure differential across restriction

z	=	Elevation
Q_v	=	Volume flow rate
C_d	=	Discharge coefficient
ε	=	Absolute roughness
C_g	=	Coefficient of geometry
Re	=	Reynolds number
μ	=	Dynamic Viscosity
ΔP_4	=	Pressure differential across straight pipe

References

1. http://www.bluewaterpetroleum.com/index.php/why_heavy_oil/definition_of_heavy_oil/69
2. NEL, *Flow Measurement in Challenging Fluids*, Report No. 2006/236, July 2006
3. NEL, *An Investigation into the Effects of High Viscosity on Conventional Flow Meters*, Report no. 2008/76, April 2008
4. Stobie, G. et al, *Erosion in a Venturi meter with Laminar and Turbulent Flow and Low Reynolds Number Discharge Coefficient Measurements*, 25th NSF MW, October 2007
5. Hollingshead, C.L., *Discharge Coefficient Performance of Venturi, Standard Concentric Orifice Plate, V-Cone and Wedge Flow Meters at Low Reynolds Numbers*, Journal of Petroleum Science and Engineering 78 (2011) 559-566
6. Melendez, G. et al, *Wedge Meters with Low Reynolds Number Flow*, FLOMEKO 2016, September 2016.
7. Rabone, J. et al, *Prognosis Applied to High Viscosity Flows*, South East Asia Flow Measurement Conference, March 2014.
8. British Standards Institute, *BS EN ISO 5167-2:2003 Measurement of fluid flow by means of differential pressure devices inserted in circular cross-section conduits running full – Part 2: Orifice plates*, 1 March 2003
9. International Standards Organisation, *ISO/TR 15377:2007 – Measurement of fluid flow by means of pressure-differential devices – Guidelines for the specification of orifice plates, nozzles and Venturi tubes beyond the scope of ISO 5167*, 2007
10. Melendez, G. et al, *Wedge Meters with Low Reynolds Number Flow*, FLOMEKO, September 2016.
11. Marshall, C., *Summary Report for ICUR Market Research Project*, Report no. 2017/406 v2, June 2017.
12. P. Jakubenas, "Measuring Flow of High Viscosity Liquids (FMC Technologies Measurement Solutions)," *Pipeline & Gas Journal*, 2007.

Figures

LIGHT OIL	45.5°
	31.1°
	30.2°
MEDIUM	22.3°
	21.5°
HEAVY	10.0°
	6.5°
EXTRA-HEAVY	0.1°

Figure 1: Classifications of Oil

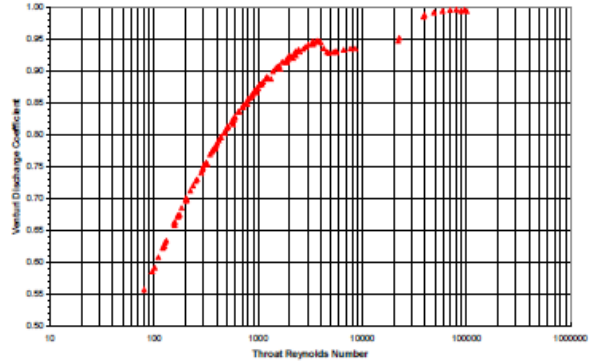


Figure 2: Typical discharge coefficient versus Reynolds number relationship

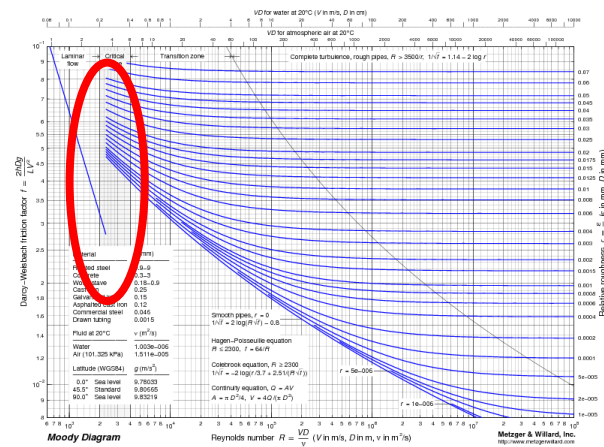


Figure 3: Darcy-Weisbach friction factor versus Reynolds number

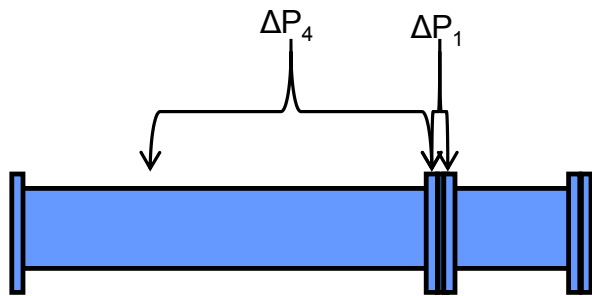


Figure 4: Orifice plate installed in a typical metering run (flow from left to right)

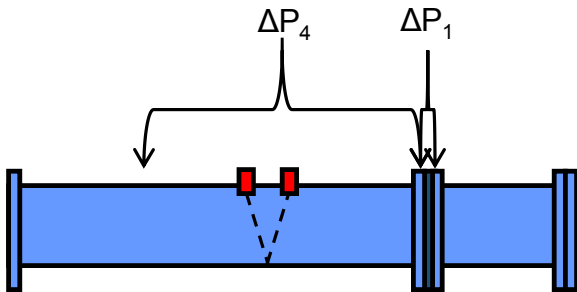


Figure 5: Orifice plate with additional clamp-on ultrasonic measurement (in red) upstream of primary element (flow left to right)

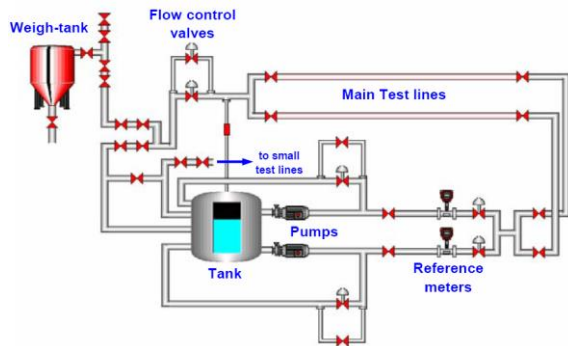


Figure 6: Schematic Diagram of the NEL Oil Flow Test Facility

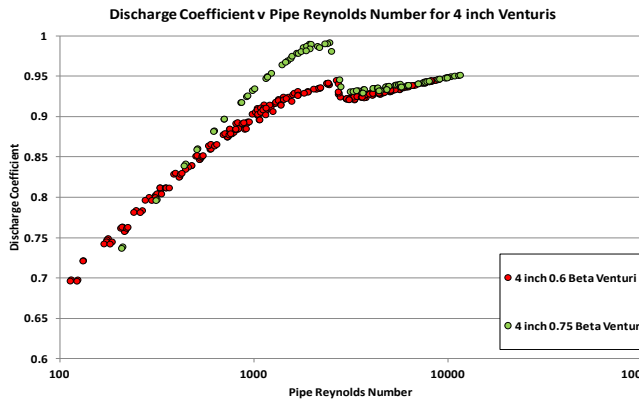


Figure 7: Discharge coefficient versus Reynolds number for 4 inch Venturis

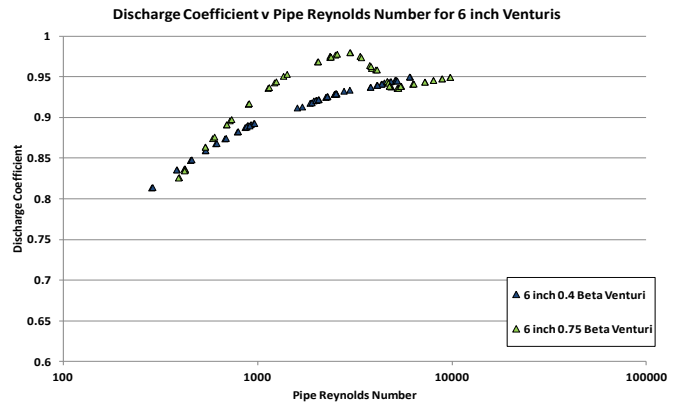


Figure 8: Discharge coefficient versus Reynolds number for 6 inch Venturis

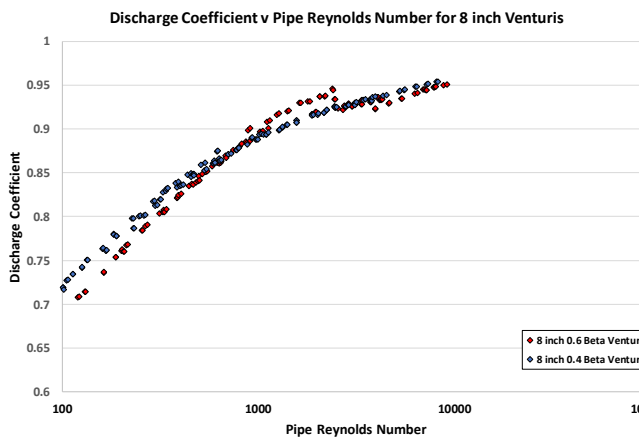


Figure 9: Discharge coefficient versus Reynolds number for 8 inch Venturis

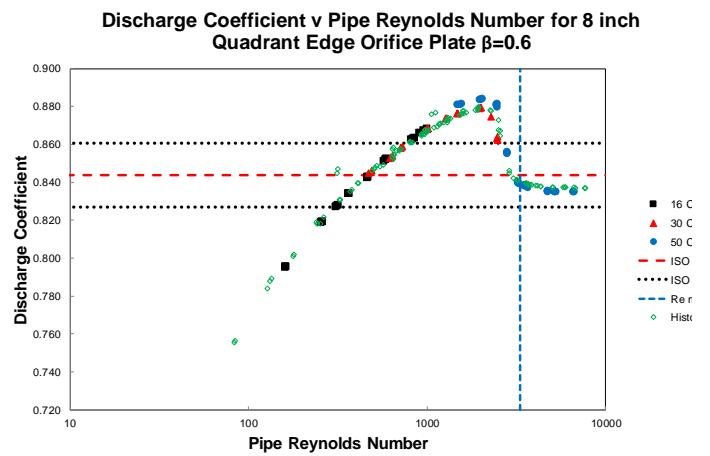


Figure 10: Discharge coefficient versus Reynolds number for 8 inch $\beta=0.6$ QE orifice plate

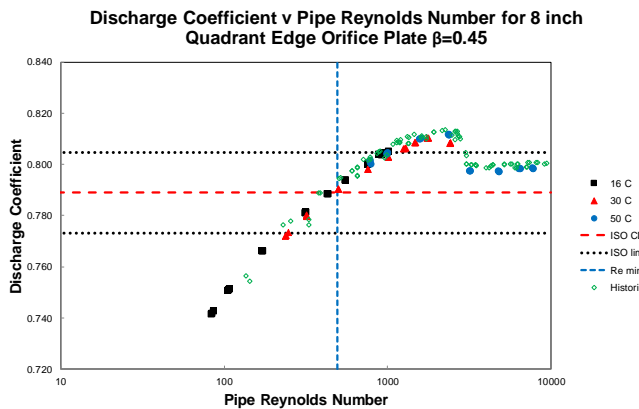


Figure 11: Discharge coefficient versus Reynolds number for 8 inch $\beta=0.45$ QE orifice plate

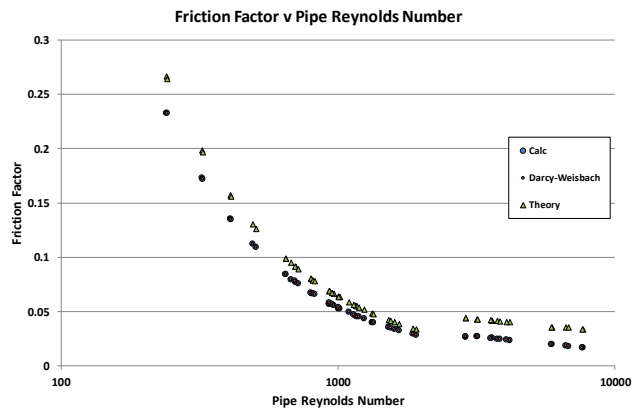


Figure 12: Friction factor versus Reynolds number for three different calculation methods

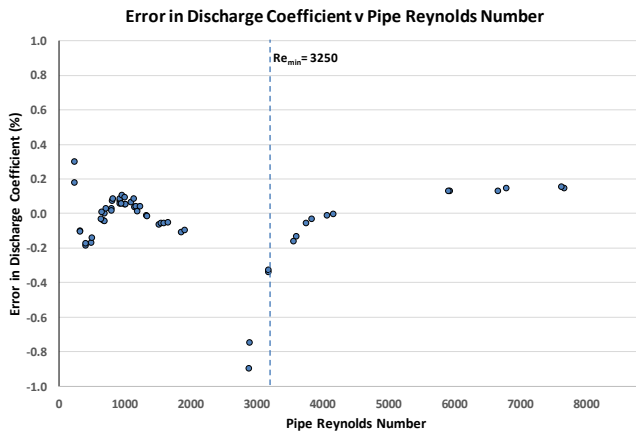


Figure 13: Error in discharge coefficient versus Reynolds number for 8 inch $\beta=0.6$ quadrant edge orifice plate

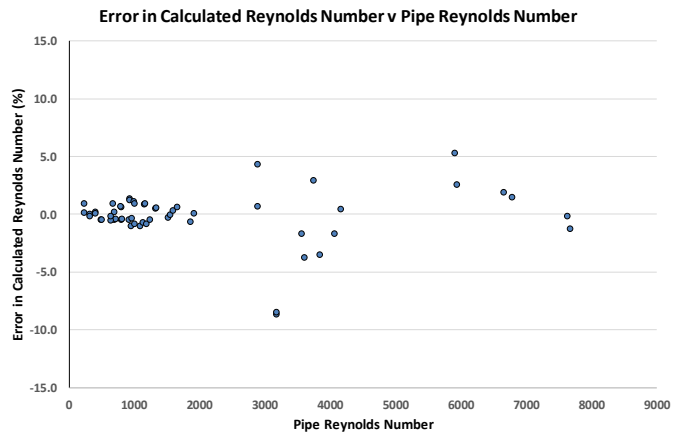


Figure 14: Error in calculated Reynolds number versus Reynolds number for 8 inch $\beta=0.6$ quadrant edge orifice plate

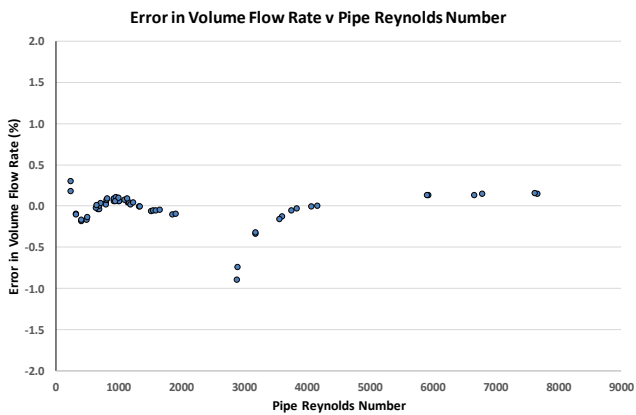


Figure 15: Error in volume flow rate versus Reynolds number for 8 inch $\beta=0.6$ quadrant edge orifice plate

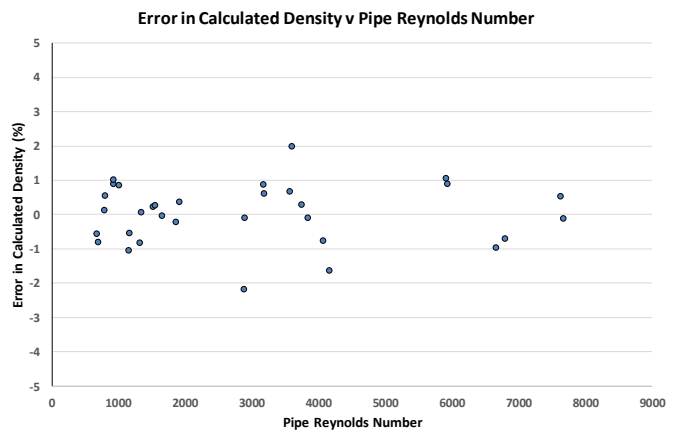


Figure 16: Error in calculated density versus Reynolds number for 8 inch $\beta=0.6$ quadrant edge orifice plate

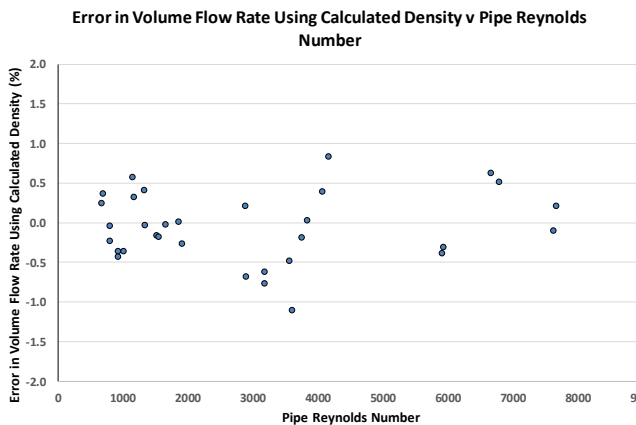


Figure 17: Error in volume flow rate using calculated density versus Reynolds number for 8 inch $\beta=0.6$ quadrant edge orifice plate

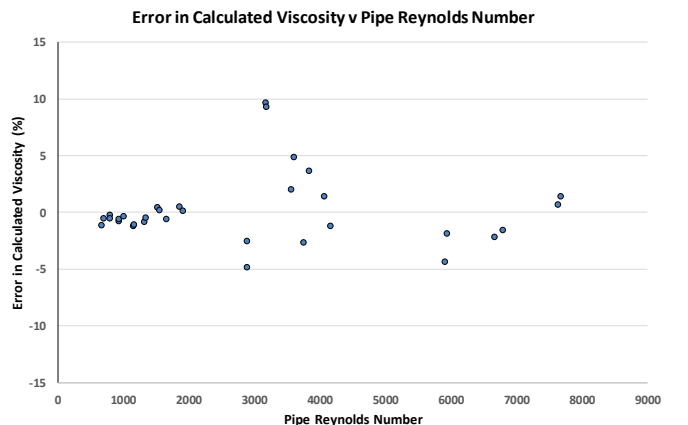


Figure 18: Error in calculated viscosity versus Reynolds number for 8 inch $\beta=0.6$ quadrant edge orifice plate